Bioengineering

AIMS Bioengineering, 8(1): 112–129.
DOI: 10.3934/bioeng.2021011
Received: 01 November 2020
Accepted: 19 January 2021
Published: 05 February 2021

http://www.aimspress.com/journal/Bioengineering

Research article

Electrospinning of chitosan from different acid solutions

Sergio A. Salazar-Brann[1], Rosalba Patiño-Herrera[1], Jaime Navarrete-Damián[2] and José F. Louvier-Hernández[1,*]

[1] Department of Chemical Engineering, National Technology of Mexico/Technological Institute of Celaya, Antonio Garcia Cubas 600, Celaya, Guanajuato 38010, Mexico
[2] Department of Equipment Design, National Technology of Mexico/CRODE Celaya, Diego Arenas Guzman 901, Celaya, Guanajuato 38020, Mexico

*** Correspondence:** Email: francisco.louvier@itcelaya.edu.mx; Tel: +524616117575.

Abstract: Electrospinning is a production technique for obtaining polymer nanofibers relatively low-cost and straightforward to produce fine fibers. Chitosan (CTS) is a well-known biopolymer widely used for drug delivery, hydrogels, tissue engineering, wound healing, and mats. This work aims to study different chitosan-organic acid solutions' conductivity using electrochemical impedance spectroscopy and equivalent circuit fitting to understand this parameter's influence in the electrospinning process for fiber formation in different organic acids as solvents. The conductivity of dilute chitosan solutions decreases until reaching a minimum value as chitosan concentration increases; conductivity increases linearly as concentration increases. We measured solution resistance, polarization resistance, and relaxation time of chitosan solutions in acetic, formic, lactic, and citric acids using electrical impedance spectroscopy with equivalent circuit modeling. There is no direct correlation between the electrospinnability of the different organic acids solutions with their solution conductivity. We obtained chitosan nanofibers and particles when electrospun a chitosan concentrated solution (4 wt%) in concentrated acetic acid (90 vol%) and obtained submicron particles with a more diluted solution (1 wt%) in concentrated acetic acid (90 vol%). We also obtained chitosan particles from formic acid solutions and completely different ordered and elongated particles with citric acid solutions. Getting insight into the organic acid-chitosan interactions will help improve the electrospinning process to obtain fibers, particles, or both in a controlled fashion and may help design tailored materials.

Keywords: acetic acid; formic acid; lactic acid; citric acid; chitosan; electrospinning; impedance spectroscopy; equivalent circuit fitting; conductivity

1. Introduction

Nanomaterials are materials within the nanometer scale, at least in one dimension. Particles, sheets, tubes, and fibers can be produced at the nanoscale. A wide variety of materials can form fibers for several industrial applications (catalysts [1], filters [2], energy storage [3], capacitors [4], and optics [5]), consumer goods (food packaging [6] and personal healthcare [7]), or biomedical applications (tissue engineering [8], immunosensing [9], dialysis membranes [10], wound healing [11], or drug delivery [12]). Different techniques can produce fibers, and electrospinning is a relatively low-cost fiber production technique and straightforward to produce fine fibers. A typical electrospinning setup includes a dosing pump with a syringe with a polymer solution inside that is injected into a high-voltage electric field formed between the syringe needle and a collector plate (or collector drum). A drop of the polymer solution forms the so-called Taylor cone at the tip of the needle, which is distorted under the electric field's action, which draws the droplet towards the collector plate, the solvent evaporates, and the fibers form as the polymer solidifies [13].

Chitin (CTN) and chitosan (CTS) are well-known biopolymers widely used in different areas such as water purification [14], biosorbent [15], catalysis [16], fuel-cells technology [17], sensors[18], and biomedicine. Biomedical chitosan-related papers include drug delivery [19], hydrogels [20], tissue engineering [21], wound healing [22,23], and mats [24]. Chitosan is a natural, non-toxic, non-expensive, biocompatible, and renewable material found in the exoskeleton of crabs and shrimps [25], or even from some insects [26]. It is classified as GRAS by the FDA [27] and is soluble at acidic pH; the most common solvent used is aqueous acetic acid 1.0 vol% [28].

Until now, it has not been reported a successful electrospun of chitosan fibers from dissolution in diluted acetic acid (i.e., at 1.0 vol% acetic acid). There are only reports of chitosan fibers obtained by mixing CTS with polyvinyl alcohol (PVA) and graphene oxide for advanced biocompatible and antibacterial biomaterials for cell culture [29], CTS with polylactic acid (PLA) for improving mechanical properties for surgical sutures or implantable devices [30]; CTS with nylon-6 for papain purification from raw papain as opposed from solubilized papain extracts[31]; CTS with PVA and carbon nanotubes (CNT) as scaffolds for cardiomyocytes differentiation in tissue engineering[21]; or CTS with polyethylene oxide (PEO) for novel biomaterials for drug dosage [32], non-woven fiber mats for air and water filtration systems [33], and biomedical, food, pharmaceutical, and other toxic-free solvent applications [34]. Also, there are reports of pure CTS fibers obtained by diluting CTS in special solvents such as trifluoroacetic acid (TFA) [35,36,30]; mixtures of trifluoroacetic acid and dichloromethane (TFA/DCM) [37]; concentrated formic acid [38]; hexafluoroisopropanol mixed with formic acid (HFIP/FA) [31]; or concentrated acetic acid (> 70 vol%) [39,40]. However, such solvents may be toxic and require a subsequent solvent-removal process that might affect the obtained nanostructure.

A recent review on electrospun polymeric nanofibers indicates that polymer solution conductivity influences the fiber formation; as conductivity increases, the fiber diameter decreases and vice versa [41]. Solutions with low conductivity, however, will not have enough charge to be electrospinnable [13]. Our interest is to study chitosan dissolution conductivity when dissolved in different organic acid solvents at different concentrations. This work aims to study chitosan-organic acid solutions' conductivity using electrochemical impedance spectroscopy and equivalent circuit fitting to understand this parameter's influence in the electrospinning process for fiber formation comparing different organic acids (acetic, formic, lactic, and citric) as solvents for dilute and concentrated acid solutions.

2. Materials and methods

2.1. Reagents

Glacial acetic acid (Fermont), formic acid (88% JT Baker), anhydrous citric acid (JT Baker), and lactic acid (85%, Karal) were used without further purification. Low molecular weight chitosan was purchased from Sigma-Aldrich (MW = 50,000–190,000 g/mol; DD = 94.3%; Batch No. MKBL7900V, CAS 9012-76-4). The intrinsic viscosity of 390.11 mL/g was measured using the Mark-Houwink relation with constants reported by Rinaudo et al. [42] in a mixture solvent of 0.3 M acetic acid/0.2 M sodium acetate to avoid aggregate formation; the viscous average molecular weight is 68,968 g/mol. The degree of deacetylation was determined as 90.4% measured by UV-Vis first derivative method.

2.2. Intrinsic viscosity

Intrinsic viscosity was determined using a Cannon-Fenske routine viscometer (Cannon, USA) in a water bath (Polyscience, AP29VB5R, USA) with a controlled temperature of 25 ± 0.02 ℃. Viscous average molecular weight is determined using K = 0.082 mL/g, and a = 0.76. Chitosan was dissolved into a mixture of 0.3 M acetic acid/0.2 M sodium acetate to obtain 0.5, 0.4, 0.3, 0.2, and 0.1 g/dL dissolutions.

2.3. Degree of deacetylation

The degree of deacetylation was determined using the first derivative method of Tan et al. [43] using D-glucosamine and N-acetylglucosamine as references and measuring UV-Vis absorption from 190 to 250 nm with a spectrophotometer (Perkin Elmer, Lambda2, USA).

2.4. Conductivity measurements

We measured conductivity and pH of chitosan solutions (see Figure S-1) at a fixed organic acid concentration (1.0 M) and different chitosan concentrations (0, 0.2, 0.4, 0.6, 0.8, 1.0, 2.0, 3.0, 4.5, 7.5, 9.0, and 15 mg/mL) with a Horiba (Laqua F-74BW, Japan) conductometer at 25 ℃ using an electrode with a measurement range of 1–100 mS/m. Conductometer calibration was done according to American Society of Testing Materials D1125-95 [44] using KCl solutions prepared in our laboratory.

2.5. Electrochemical impedance spectroscopy

The impedance of solutions of the experimental design was measured using a potentiostat/galvanostat (Ametek Princeton Applied Research, model 263A, USA) coupled with a Lock-in amplifier (Ametek Signal Recovery, model 5210, USA) in a typical three-electrode glass cell with a copper working electrode with a surface area of 0.126 cm^2, a platinum counter-electrode, and a calomel reference electrode in a frequency range from 0.1 to 10 kHz with an amplitude voltage of 10 mV. Similar procedures have been applied but to chitosan solid films [45,46].

2.6. Equivalent circuit

The complex electrical impedance results of the solutions are fitted using the equivalent circuit shown in Figure 1, which consist of a resistance, R_s, coupled in series with a constant phase element (CPE) in parallel with a second resistance, R_{pol}, element. A complex fitting was performed with the Zview software.

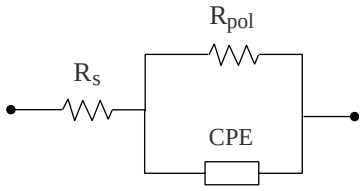

Figure 1. Equivalent circuit proposed to describe experimental impedance data of acetic acid-water solutions.

The first resistance, R_s, is the high-frequency resistance associated with solution resistance. The second resistance, R_{pol}, is associated with the electrode polarization resistance. However, a resistance and a capacitor in parallel do not describe the system's behavior; hence a CPE is used in place of a capacitor defined by two values, τ_0, and n, to compensate for non-homogeneity due to working electrode roughness, porosity, and geometry. If $n = 1$, then the equation is that of a capacitor; if $n = 0.5$, then a 45 °line is produced in the Nyquist plot and describes a diffusion mechanism. The following complex relation gives the impedance of the equivalent fractional-order circuit

$$Z(\omega) = R_s \frac{R_{pol}}{1 + (j\omega\tau_0)^n} \tag{2.1}$$

where Z is the complex impedance, R_s is the resistance of the solution, R_{pol}, is the polarization resistance, τ_0, is the relaxation time, and n, the parameter that accounts for the deformation of the semicircle or the effects associated to the constant phase element, such as interfacial ion mobility features. For example, the non-ideal double layer's capacitance due to non-homogeneous adsorption in a rough or porous electrode surface will appear as a CPE with n values between 0.9–1.0. Cell constant determination was performed by calibrating the cell using KCl solutions at three different concentrations 0.01 M, 0.1 M, 1.0 M. Our setup is not temperature controlled, and all the experiments were done at room temperature.

2.7. Electrospinning

We performed electrospinning experiments using the in-house made apparatus of Figure 2, following similar procedures previously reported [10,47] with a dosing pump that pushes polymer solution contained in a syringe through a 0.500-micron needle. The electric field is formed between two circular copper plates connected to a high-voltage supply. Voltage was set to 18 kV, with a plate distance of 12.5 cm, and a polymer solution flow of 1.5 mL/h for three hours. Temperature and relative humidity are not controlled, but we recorded these two variables (Table S-1).

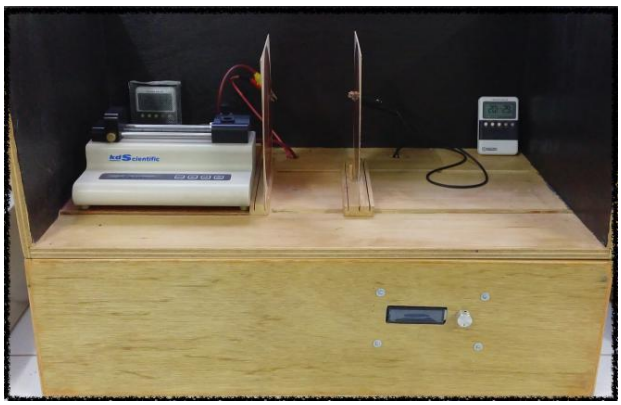

Figure 2. In-house made electrospinning apparatus.

We proposed two factors for each organic acid with two levels: acid concentration and chitosan concentration. The low level of organic acid concentration was decided regarding the most common concentration, i.e., the usual solvent for chitosan is acetic acid at 1.0 vol% concentration. For the high level of organic acid concentration, we decided to use 90 vol% since there is evidence of chitosan fiber formation using this solvent [39]. Low (1.0 vol%) and high (4.0 vol%) chitosan concentration levels were decided as the typical values for chitosan dissolution (low) and to cover most of the possible dissolution range (high). Design of experiments consist of sixteen samples, each experiment was performed by duplicate.

2.8. Characterization

Fiber morphology is evaluated using a Scanning Electronic Microscope (JEOL, JSM-6510LV, Japan) at a constant voltage of 20 kV. Samples were sputter-covered with a gold film with a coating system (DentonVacuum, Desk V, USA) at 0.1 mbar and 28 mA.

Statistical analysis was performed using the DoE analysis function of Minitab and surface contour plots for conductivity, polarization resistance, relaxation time, and parameter *n* of the equivalent circuit fitting results.

3. Results

3.1. Conductivity

Figure 3 shows conductivity behavior as a function of chitosan concentration in different organic acids (1.0 M). As chitosan concentration increases, conductivity first decreases until reaching a minimum value and then increases with a linear behavior. The overall behavior of chitosan conductivity in formic, acetic, and lactic aqueous solutions is very similar. The minimum conductivity value for acetic acid is reached at about 0.6 mg/mL, while the minimum for formic acid is reached at about 2 mg/mL, for lactic acid at about 3 mg/mL, and the minimum conductivity for the citric acid solvent is reached at about 9 mg/mL chitosan concentration. Li et al. [48] already observed this behavior for weak acids, and our results for acetic and formic acids are in good agreement with theirs. Aqueous organic weak acids dissociate into carboxylic acid ions ($RCOO^-$) and hydrogen ions (H_3O^+),

but there are also acid molecules (RCOOH) and water molecules (H_2O) in solution. Chitosan dissolves into the aqueous acid by binding to the hydrogen ions, as depicted by Rinaudo et al. [42].

$$CTS{-}NH_2 + RCOO^- + H_3O^+ \rightleftharpoons CTS{-}NH_3^+ + RCOO^- + H_2O \quad (3.1)$$

where CTS stands for the glucosidic residue of chitosan chain. pH increases monotonically as chitosan concentration increases for all organic acids (Figure 4).

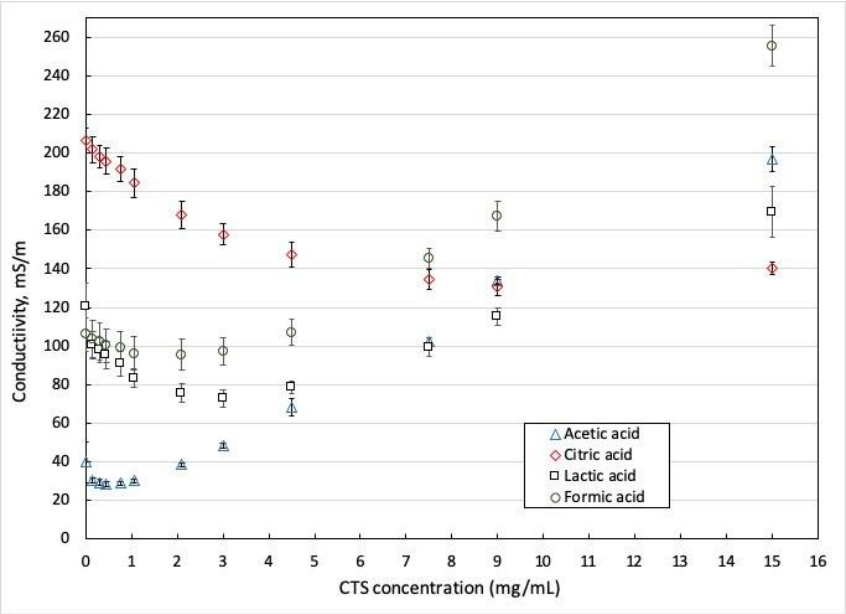

Figure 3. Conductivity of chitosan solutions for different weak organic acids at 1.0 M.

It is attributed to the dissolution mechanism by protonation of chitosan amino groups, which will decrease the hydrogen ions in the solution causing an increase in pH. The counterion formed depends on the acid used (i.e., acetate, formate, lactate, or citrate ion), and chitosan acts as a polyelectrolyte. Li et al. [48] explained the minimum in conductivity as follows: first when chitosan binds to hydrogen ions, conductivity decreases slightly (the first decrease at low chitosan concentration) because the free ions are responsible for charge transport, and the chitosan chains tend to conform in an extended chain because of electrostatic repulsion of the positive charges along its backbone. When dissociated hydroniums are bound completely at increasing chitosan concentration, more chitosan begins to interact with undissociated carboxylic acid molecules by which charges are transported and conductivity increases. They also explained that, at plateau concentration of conductivity (concentration of conductivity minimum), chitosan interacts with carboxylic acid molecules and form stable and ordered complexes through cross-linking bonding of chitosan's amino groups with the carboxylic acid and hydrogen bonds between hydroxyl groups on chitosan chains with carboxylic acid molecules. They propose that carboxylic acid ions and hydronium move orderly along this complex and transport charge, which causes conductivity to increase as chitosan concentration increases (which promotes the formation of more complexes). This explanation should be carefully analyzed since they do not provide experimental evidence of the complex formation. This behavior has not been studied by anyone else to date.

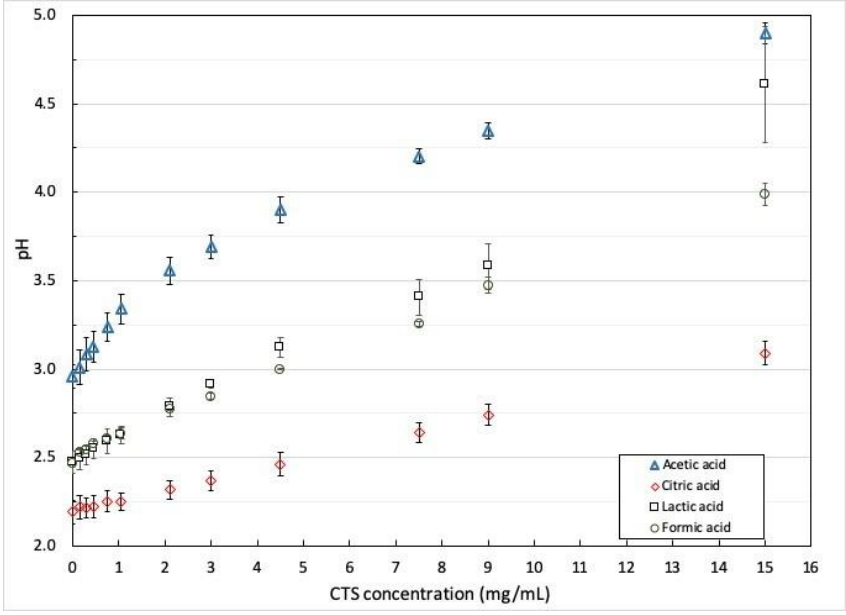

Figure 4. pH of chitosan solutions for different weak organic acids at 1.0 M.

4. Impedance measurements

We measured pH and electric conductivity to the sixteen solutions (Figure S-2) of the design of experiments, and results are shown in Table S-2. Acetic, formic, and lactic acids decrease their conductivity as their concentration increases, whereas citric acid increases its conductivity as its concentration increases. Another feature is that when increasing chitosan concentration, conductivity increases in all organic acids except for citric acid. Hence, citric acid behaves differently from acetic, formic, and lactic acids, probably due to the presence of three acid functional groups in citric acid. pH behaves as expected, it increases as chitosan concentration increases due to the binding of hydronium with amino groups, and it decreases as acid concentration increases.

Impedance results can be plotted in a Nyquist plot of the real part of the impedance, Z_{re}, versus the imaginary part of the impedance, $-Z_{im}$, usually in the positive *y*-axis. Figure 5 presents the Nyquist plot of all the experiments, and we can observe that all the samples' behavior is a depressed semicircle, and we fitted this behavior with the equivalent circuit of Figure 1. Acetic acid solutions at 1 vol% show a lower resistance than solutions at 90 vol%, and the diameter of semicircle is about 1000 Ω compared to ~1500 Ω, respectively. When increasing chitosan concentration, solution resistance decreases. Formic acid solutions at 1 vol% show a smaller semicircle diameter of about 600–700 Ω, while solutions at 90 vol% have diameters of 1500–1800 Ω, which is twice that of the lower concentration. Solution resistance, however, has similar values for all samples between 100–300 Ω. The formic acid samples' impedance plots are in the 2000 Ω range, and its behavior can be compared to that of the acetic acid at 1 vol%, where solution resistance decreases when increasing chitosan concentration.

Lactic acid solutions at 1 vol% showed a lower resistance than solutions at 90 vol%. The semicircle diameter is variable from 1200 Ω for the solution at 1 vol% lactic acid with 1 wt% chitosan to 4100 Ω for the solution 90 vol% lactic acid with 1 wt% chitosan, and solution resistance decreases as chitosan concentration increases. Finally, we found a completely different behavior for citric acid solutions. The solution with citric acid at 1 wt% and 4 wt% chitosan shows the highest semicircle

diameter value of ~6800 Ω and it is also the highest value of all the samples, while the solution with citric acid at 90 wt% and 4 wt% chitosan is the sample with the smallest diameter of about 900 Ω. Contrary to the other organic acids, solution resistance of citric acid solutions at 1 vol% is higher than solution resistance at 90 vol% citric acid concentration, and solution resistance increases when increasing chitosan concentration. Citric acid is a tricarboxylic acid with chelating properties, which might cause this utterly different behavior compared to the acetic, formic, and lactic acids.

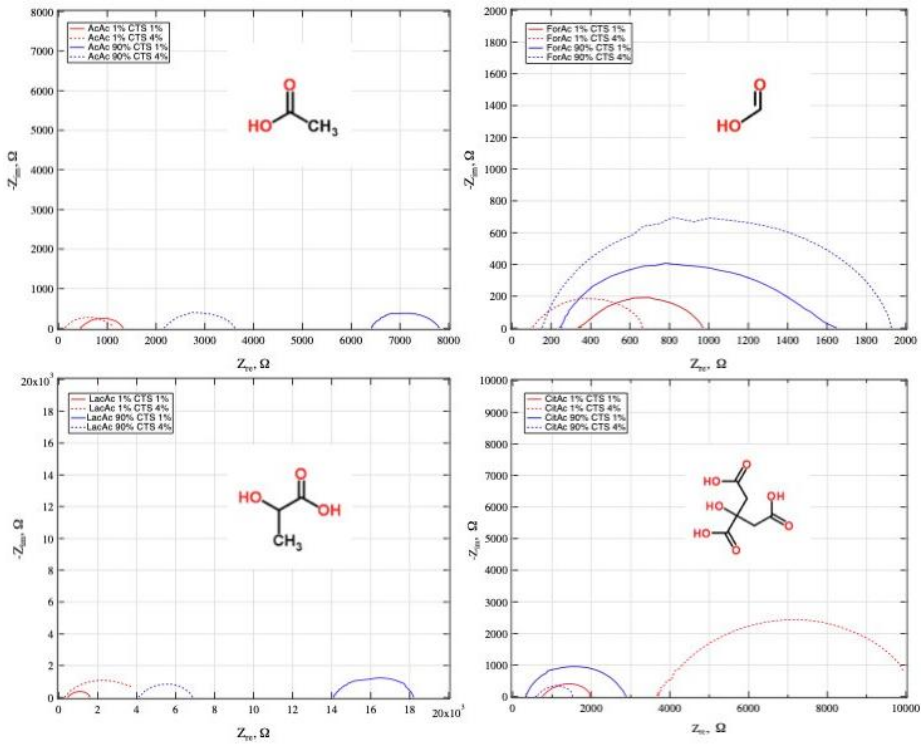

Figure 5. Nyquist plots for all the samples. Each plot corresponds to a different organic acid as solvent.

5. Electrospinning of chitosan

Electrospinning of chitosan solutions was performed in the in-house made apparatus shown in Figure 2, and electrospun fibers were taken from the collector plate using an aluminum foil previously attached to it. Electrospun samples were dried in an oven at 60 ℃ for 24 h to remove any remaining solvent.

We want to evaluate the electrospinnability of chitosan dissolved in different organic acids. We measure the area covered by the electrospun polymer's membrane over the aluminum paper to assess the solutions' fiber formation capability. Table 1 shows the membrane area measured, and it is possible to see that not all the samples form fibers. In particular, we did not obtain fibers from lactic acid solutions (not shown in the table). We observed that the droplet exiting the needle traveled through the electric field until the collector plate without evaporating the solvent and finally was deposited over the aluminum foil, forming a film. This experiment does not necessarily rule out the fiber formation using lactic acid as solvent.

Table 1. Membrane area obtained after electrospinning for different solutions.

Organic acid	Acid concentration, vol%	Chitosan concentration, wt%	Membrane area, cm^2
	1	1	NA
Acetic acid	1	4	NA
	90	1	17.77(2.64)
	90	4	53.90(13.75)
	1	1	NA
Formic acid	1	4	42.59(20.03)
	90	1	20.13(18.46)
	90	4	48.40(21.52)
	1	1	NA
Citric acid	1	4	NA
	90	1	7.37(7.91)
	90	4	58.90(0)

*Note: Standard deviation in parenthesis.

The fiber mat formed over the aluminum foil showed different geometrical forms depending on the organic acid. Acetic and formic acid yielded circular mats of different diameters, while citric acid yielded ellipsoidal fiber mats. Figure 6 shows photographs for the mats obtained from acetic, formic, and citric acid solutions in frontal and lateral views. The ellipsoidal mat obtained from citric acid suggests that solution properties might influence Taylor's cone geometry, and more experiments should be done to elucidate this phenomenon.

Chitosan solutions in acetic acid 1 vol% were not apt for electrospinning; the solution at 1 wt% CTS had very low viscosity that the droplet traveled to the collector plate without forming fibers. The solution at 4 wt% was so viscous that the needle clogged at the beginning of the experiment. It is important to note that solution viscosity depends upon average molecular weight and distribution molecular weight, and it seems that a dilute acetic acid solution can dissolve less chitosan than concentrated acetic acid solutions, which are the reasons that other works can dissolve up to 7–7.5 wt% chitosan [39,40]. The morphology of the mats at the microscopy level formed from chitosan solutions in 90 vol% acetic acids are shown in Figure 7-A1-F1. There are agglomerated spherical particles at chitosan concentration of 1 wt% (A1-B1), while chitosan solution at 4 wt% yields fibers and beads with a significant formation of micron-size spherical particles (C1–D1) bonded together by nano-size fibers (E1–F1).

Chitosan solution at 1 wt% in formic acid 1 vol% was not electrospinnable because of its very low viscosity. Although the other three formic acid solutions were electrospinnable, they did not form any fiber. Chitosan solution at 1 wt% in formic acid 90 vol% yields different particle sizes, particularly Figure 7-A2 shows a big particle of size greater than 5 microns and multiple sub-micron particles around. Chitosan solutions at 4 wt% in formic acid 90 vol% and 1 wt% in formic acid 1 vol% yielded sub-micron particles with no evidence of fibers (Figure 7-B2–C2).

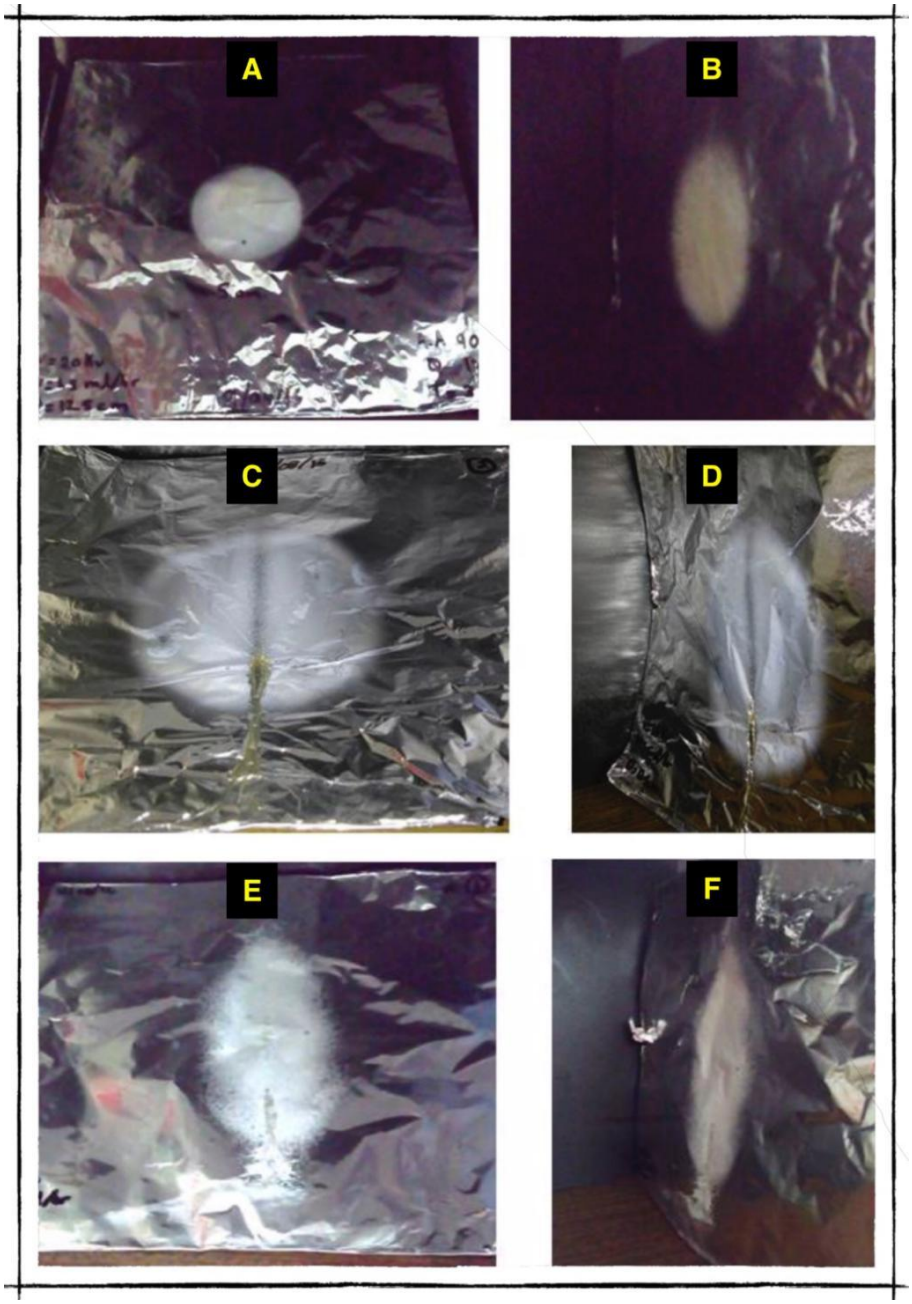

Figure 6. Fiber mats obtained from: (A) acetic acid frontal view, (B) acetic acid side view, (C) formic acid frontal view, (D) formic acid side view, (E) citric acid frontal view, and (F) citric acid side view. Note the elliptical form of the later.

Chitosan solutions in citric acid at 1 wt% were not electrospinnable either because the viscosity was very low for chitosan concentration of 1 wt%, or because chitosan did not completely dissolve at 4 wt% (Figure S-2). We discovered that mats obtained at a citric acid concentration of 90 wt% are neither fibers nor spherical particles. Figure 7-A3-B3 shows a morphology that resembles some ordered tiles, made of elongated particles. We could not get a closer zoom because the electron beam caused degradation of the samples. It is possible to observe some degradation in Figure 7-A3, when attempting to magnify the sample view. This result, along with the formed elliptical membrane, is characteristic only to citric acid samples.

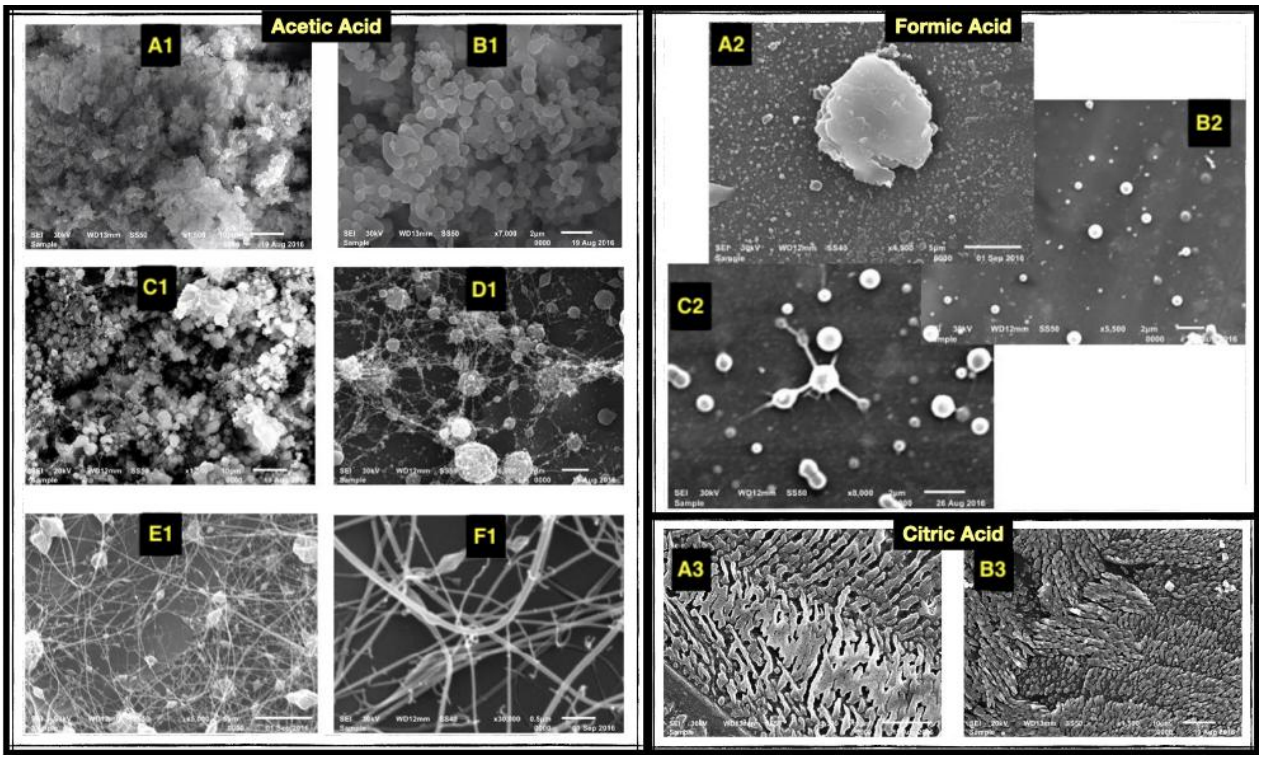

Figure 7. Micrographs from acetic acid solutions: (A1–B1) acetic acid 90 vol% and 1 wt% chitosan, (C1–F1) acetic acid 90 vol% and 4 wt% chitosan; formic acid solutions: (A2) formic acid 90 vol% and 1 wt% chitosan, (B2) formic acid 90 vol% and 4 wt% chitosan, and (C2) formic acid 1 vol% and 4 wt% chitosan; and citric acid solutions: (A3) citric acid 90 wt% and 1 wt% chitosan, and (B3) citric acid 90 wt% and 4 wt% chitosan.

6. Discussion

Solution conductivity can be determined by fitting solution resistance from the Nyquist plot and the cell constant. Contour plots of the factors analyzed for solution's conductivity are shown in Figure 8, where it can be seen that conductivities of acetic, formic, and lactic acids solutions are higher when organic acid concentration is low, and chitosan concentration is high; while is completely opposite for citric acid solution, where conductivity is higher when citric acid concentration is high, and chitosan concentration is low. There is no direct correlation between the electrospinnability of the different organic acids' solutions with their solution's conductivity.

Figure 9 shows contour plots of the factor analyzed with respect to polarization resistance. It increases as the acid concentration increases and increases as chitosan concentration increases for acetic and formic acid solutions. Lactic and citric acids have different behavior, lactic acid show higher values from low acid concentration and high chitosan concentration to high acid concentration and low chitosan concentration (with a saddle point at around 60 vol% lactic acid and 3.5 wt% chitosan). Citric acid solutions show a higher polarization resistance at low citric acid concentration and high chitosan concentration; however, chitosan was not entirely dissolved at these conditions. This experiment's lowest polarization resistance goes from low citric acid concentration and low chitosan concentration to high citric acid concentration and high chitosan concentration (with a saddle point at around 70 vol% citric acid and 1.5 wt% chitosan).

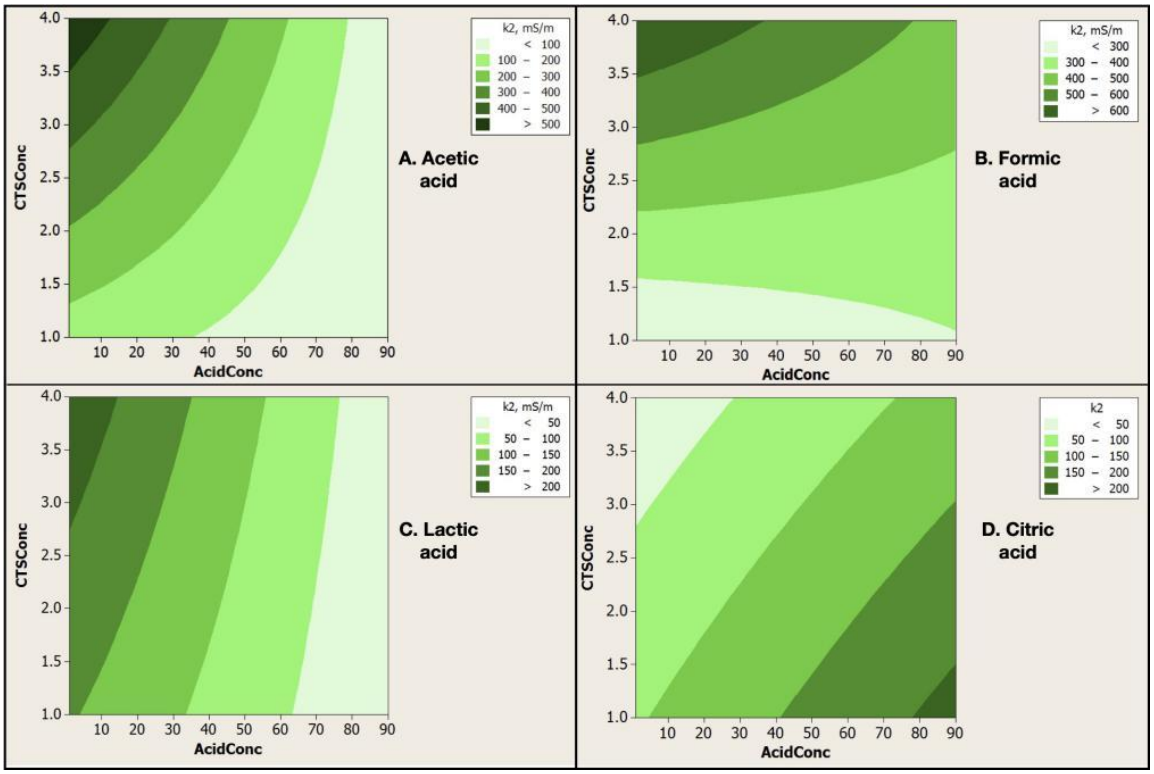

Figure 8. Contour plots for solution conductivity as a function of organic acid concentration and chitosan concentration for: (A) acetic acid solutions, (B) formic acid solutions, (C) lactic acid solutions, and (D) citric acid solutions.

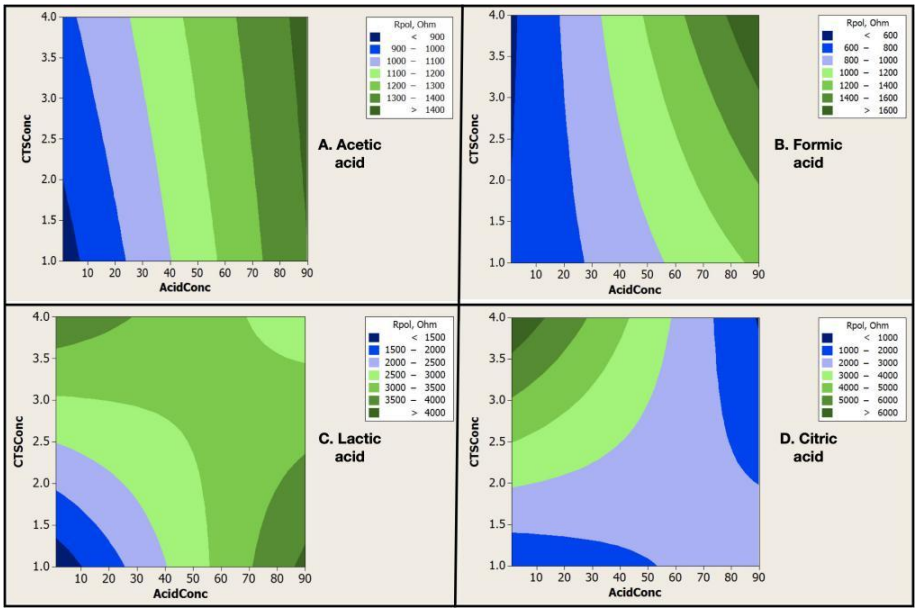

Figure 9. Contour plots for polarization resistance as a function of organic acid concentration and chitosan concentration for: (A) acetic acid solutions, (B) formic acid solutions, (C) lactic acid solutions, and (D) citric acid solutions.

Figure 10 shows contour plots of the analyzed factors for parameter *n* of the equivalent circuit model. Parameter *n* is used to compensate for the non-homogeneity of the working electrode. If $n = 1$, the solution behaves as a capacitor, but if $n = 0.5$, then it describes a diffusion mechanism. Following this concept, acetic and lactic acids solutions show a *n* value between 0.67–0.74, meaning that solutions show a diffusion character. On the other hand, formic and citric acids solutions show values of $0.75 < n < 0.86$, meaning that solutions behave more like a capacitor.

Figure 11 shows contour plots of the factor analyzed with respect to relaxation time. The highest relaxation time for all organic acids occurs at low acid concentration and high chitosan concentration. Citric and lactic acid relaxation times are one magnitude order greater than formic acid values and twice the acetic acid values. The overall behavior is similar for acetic, lactic, and citric acid relaxation times as a function of acid and chitosan concentration, whereas formic acid behaves differently. The lowest relaxation time value of formic acid solution occurs at low acid concentration and low chitosan concentration.

Figure 12 shows contour plots of the factor analyzed for membrane area. Membranes were obtained for acetic acid at high acid concentration and high chitosan concentration, for formic acid at high chitosan concentration and low and high acid concentration, for lactic acid, no membranes were obtained, and for citric acid at high acid concentration and high chitosan concentration.

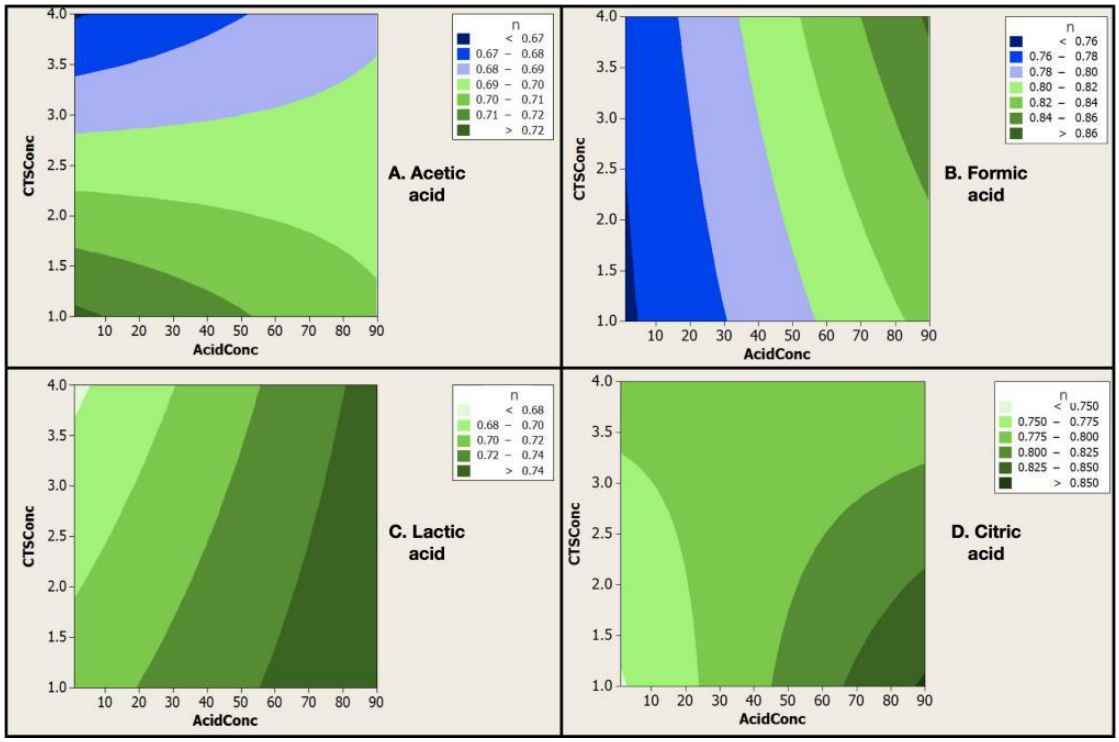

Figure 10. Contour plots for parameter *n* as a function of organic acid concentration and chitosan concentration for: (A) acetic acid solutions, (B) formic acid solutions, (C) lactic acid solutions, and (D) citric acid solutions.

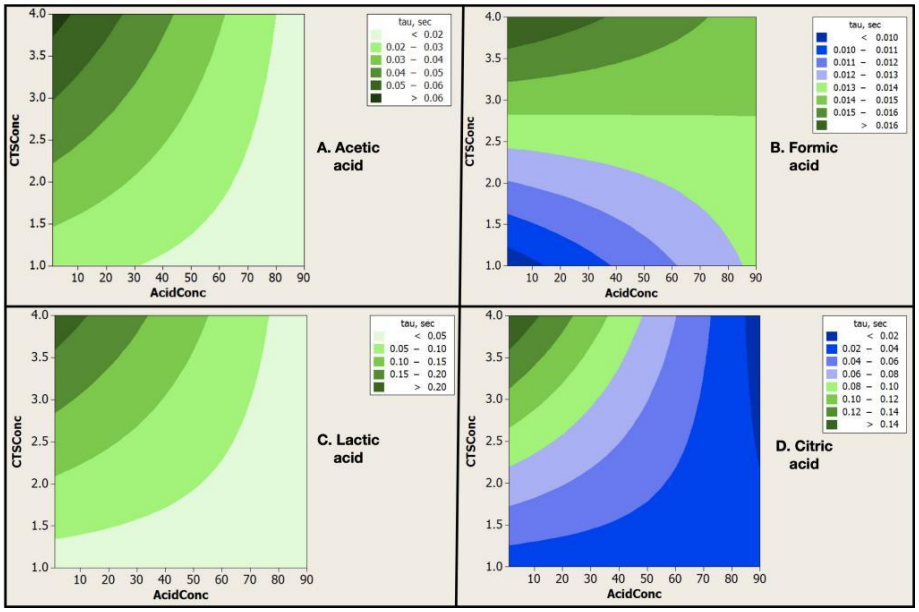

Figure 11. Contour plots for relaxation time τ as a function of organic acid concentration and chitosan concentration for: (A) acetic acid solutions, (B) formic acid solutions, (C) lactic acid solutions, and (D) citric acid solutions.

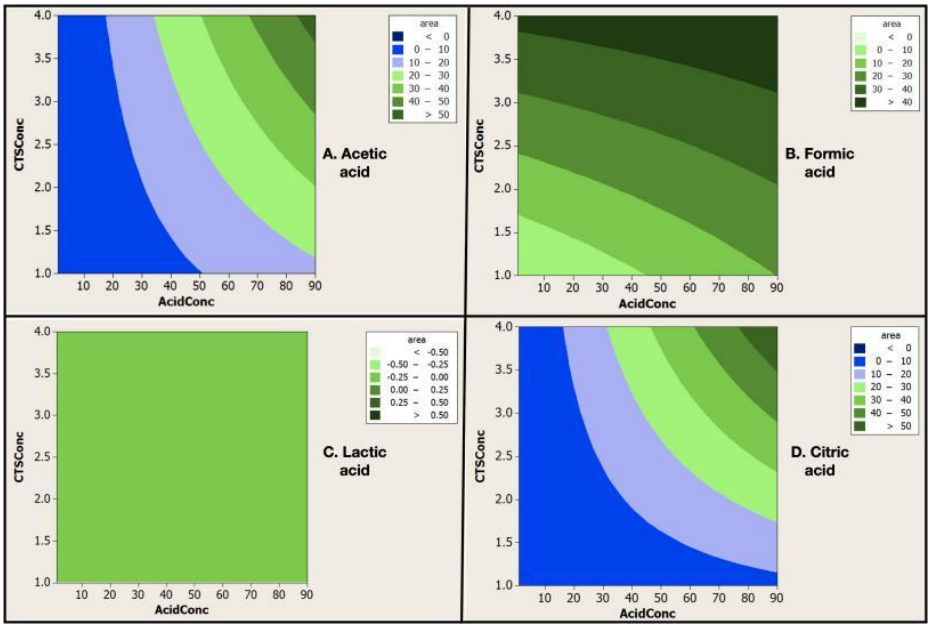

Figure 12. Contour plots for membrane area as a function of organic acid concentration and chitosan concentration for: (A) acetic acid solutions, (B) formic acid solutions, (C) lactic acid solutions, and (D) citric acid solutions.

We were able to obtain some fibers at high concentration acetic acid and high concentration chitosan, which is in good agreement with the work of Geng et al. [39] and Homayoni et al. [40]. Homayoni et al. [40] proposed to treat chitosan with alkali to reduce molecular weight through hydrolysis. They tried electrospinning with chitosan molecular weights from 1,095,000 down

to 294,000 g/mol and formed fibers dissolving 5 wt% chitosan of viscous average molecular weight 294,000 g/mol in acetic acid 90 vol% and at 7.5 wt% CTS in acetic acid 70 vol%. They explained that fiber formation at this molecular weight might be due to chains at this low molecular weight are below the threshold required for entanglement coupling formation. However, this is opposed to the concept that electrospinning can only occur with moderately concentrated solutions, as the process of jet formation relies on the entanglement of the chains [49].

Geng et al. [39] successfully electrospun chitosan dissolved at 7 wt% in acetic acid 90 vol% with an average molecular weight of 106,000 g/mol. They formed fibers and beads even at acetic acid concentrations of 30 vol%, indicating that the electric field should be higher than 3 but lower than 5 kV/cm. They consider that surface tension depression produced by the increase in acetic acid concentration is the most important solution factor that influences chitosan electrospinning. They also used chitosan with average molecular weights of 30,000 and 398,000 g/mol, and state that when using 30,000 g/mol chitosan, only fragile fibers with several droplets were obtained; we used here a 69,000 g/mol chitosan and probably have the same behavior as them.

We attempted to correlate the solution's conductivity with electrospun's ability but did not find any correlation. Acetic acid 90 vol% had very low conductivity and formed fibers and beads. However, lactic acid 90 vol% and citric acid 1 wt% also had low conductivity (below 150 mS/m) and were not able to electrospun due to the solutions' low viscosity or the inability of the solvent to evaporate. In the electrospinning apparatus, we used two circular plates to produce uniform and parallel field lines of the electric field as a new feature instead of using the tip of the needle and the collector plate, as is more commonly reported. We believe that the parallel plates reduce the needle tip's charge density and uniformly distribute the field lines over the circular plate. However, the electrospinning process may take advantage of the high charge density at the needle tip to form Taylor's cone in the traditional set-up. More experiments are needed to understand that phenomenon.

7. Conclusions

Conductivity at a very low chitosan concentration of all organic acids showed a minimum value that is still not completely understood. It is necessary to perform more experiments to elucidate this behavior.

We measured solution resistance using electrical impedance spectroscopy and adjusted experimental data with equivalent circuit modeling. Solution conductivity, polarization resistance, *n* parameter, and relaxation time can be calculated from the equivalent circuit fitting and can provide more information about the electrical interactions between all solution components: water, acid, and polymer. There is no direct correlation between the electrospinnability of the different organic acid solutions with their solution's conductivity.

We obtained chitosan nanofibers and particles when electrospun a chitosan concentrated solution (4 wt%) in concentrated acetic acid (90 vol%) and obtained sub-micron particles with a more diluted solution (1 wt%) in concentrated acetic acid (90 vol%). We also obtained chitosan particles from formic acid solutions. A completely different ordered and elongated particles were obtained with citric acid solutions. Getting insight into the organic acid-chitosan interactions will help improve the electrospinning process to obtain fibers, particles, or both in a controlled fashion and may help design tailored materials, such as non-woven fiber mats for air and water filtration systems, advanced biocompatible and antibacterial biomaterials for cell culture, improved mechanical properties for

surgical sutures or implantable devices, scaffolds for tissue engineering, or novel biomaterials for drug dosage, and other toxic-free solvent applications.

Acknowledgments

We want to thank Conacyt for the scholarship for Sergio Alejandro Salazar-Brann.

Conflict of interest

Authors declare no conflict of interest.

References

1. Ghorbani-Choghamarani A, Taherinia Z, Heidarnezhad Z, et al. (2020) Application of nanofibers based on natural materials as catalyst in organic reactions. DOI: org/10.1016/j.jiec.2020.10.028.
2. Phan DN, Khan MQ, Nguyen NT, et al. (2021) A review on the fabrication of several carbohydrate polymers into nanofibrous structures using electrospinning for removal of metal ions and dyes. *Carbohyd Polym* 252: 117175.
3. Liu M, Deng N, Ju J, et al. (2019) A review: electrospun nanofiber materials for lithium-sulfur batteries. *Adv Funct Mater* 29: 1905467.
4. Wang H, Niu H, Wang H, et al. (2021) Micro-meso porous structured carbon nanofibers with ultra-high surface area and large supercapacitor electrode capacitance. *J Power Sources* 482: 228986.
5. Zhang L, Tang Y, Tong L (2020) Micro-/nanofiber optics: Merging photonics and material science on nanoscale for advanced sensing technology. *Iscience* 23: 100810.
6. Aytac Z, Huang R, Vaze N, et al. (2020) Development of biodegradable and antimicrobial electrospun zein fibers for food packaging. *ACS Sustain Chem Eng* 8: 15354–15365.
7. Feng X, Li J, Zhang X, et al. (2019) Electrospun polymer micro/nanofibers as pharmaceutical repositories for healthcare. *J Control Release* 302: 19–41.
8. Ngadiman NHA, Yusof NM, Idris A, et al. (2017) Development of highly porous biodegradable γ-Fe_2O_3/polyvinyl alcohol nanofiber mats using electrospinning process for biomedical application. *Mater Sci Eng C* 70: 520–534.
9. Horne J, McLoughlin L, Bridgers B, et al. (2020) Recent developments in nanofiber-based sensors for disease detection, immunosensing, and monitoring. *Sensor Actuat Rep* 2: 100005.
10. Haghdoost F, Bahrami SH, Barzin J, et al. (2021) Preparation and characterization of electrospun polyethersulfone/polyvinylpyrrolidone-zeolite core–shell composite nanofibers for creatinine adsorption. *Sep Purif Technol* 257: 117881.
11. Zhao Y, Qiu Y, Wang H, et al. (2016) Preparation of nanofibers with renewable polymers and their application in wound dressing. DOI: org/10.1155/2016/4672839.
12. Parham S, Kharazi AZ, Bakhsheshi-Rad HR, et al. (2020) Electrospun nano-fibers for biomedical and tissue engineering applications: A comprehensive review. *Materials* 13: 2153.
13. Haider A, Haider S, Kang IK (2018) A comprehensive review summarizing the effect of electrospinning parameters and potential applications of nanofibers in biomedical and biotechnology. *Arab J Chem* 11: 1165–1188.

14. Rezaei Soulegani S, Sherafat Z, Rasouli M (2021) Morphology, physical, and mechanical properties of potentially applicable coelectrospun polysulfone/chitosan-polyvinyl alcohol fibrous membranes in water purification. *J Appl Polym Sci* 138: 49933.
15. Sarode S, Upadhyay P, Khosa MA, et al. (2019) Overview of wastewater treatment methods with special focus on biopolymer chitin-chitosan. *Int J Biol Macromol* 121: 1086–1100.
16. Lee M, Chen BY, Den W (2015) Chitosan as a natural polymer for heterogeneous catalysts support: a short review on its applications. *Appl Sci* 5: 1272–1283.
17. Ma J and Sahai Y (2013) Chitosan biopolymer for fuel cell applications. *Carbohyd Polym* 92: 955–975.
18. Nasr A, Gawad SA, Fekry AM (2020) A sensor for monitoring the corrosion behavior of orthopedic drug calcium hydrogen phosphate on a surgical 316L stainless steel alloy as implant. *J Bio/Tribo-Corros* 6: 36.
19. Dizaji BF, Azerbaijan MH, Sheisi N, et al. (2020) Synthesis of PLGA/chitosan/zeolites and PLGA/chitosan/metal organic frameworks nanofibers for targeted delivery of Paclitaxel toward prostate cancer cells death. *Int J Biol Macromol* 164: 1461–1474.
20. Nitta S, Kaketani S, Iwamoto H (2015) Development of chitosan-nanofiber-based hydrogels exhibiting high mechanical strength and pH-responsive controlled release. *Eur Polym J* 67: 50–56.
21. Mombini S, Mohammadnejad J, Bakhshandeh B, et al. (2019) Chitosan-PVA-CNT nanofibers as electrically conductive scaffolds for cardiovascular tissue engineering. *Int J Biol Macromol* 140: 278–287.
22. Bayat S, Amiri N, Pishavar E, et al. (2019) Bromelain-loaded chitosan nanofibers prepared by electrospinning method for burn wound healing in animal models. *Life Sci* 229: 57–66.
23. Qiu H, Zhu S, Pang L, et al. (2020) ICG-loaded photodynamic chitosan/polyvinyl alcohol composite nanofibers: Anti-resistant bacterial effect and improved healing of infected wounds. *Int J Pharmaceut* 588: 119797.
24. Kalantari K, Afifi AM, Jahangirian H, et al. (2019) Biomedical applications of chitosan electrospun nanofibers as a green polymer–Review. *Carbohyd Polym* 207: 588–600.
25. Kurita K (2006) Chitin and chitosan: functional biopolymers from marine crustaceans. *Mar Biotechnol* 8: 203–226.
26. Kaya M, Akyuz B, Bulut E, et al. (2016) Chitosan nanofiber production from Drosophila by electrospinning. *Int J Biol Macromol* 92: 49–55.
27. Wang W, Meng Q, Li Q, et al. (2020) Chitosan derivatives and their application in biomedicine. *Int J Mol Sci* 21: 487.
28. Rinaudo M (2006) Chitin and chitosan: Properties and applications. *Prog Polym Sci* 31: 603–632.
29. Liu Y, Park M, Shin HK, et al. (2014) Facile preparation and characterization of poly (vinyl alcohol)/chitosan/graphene oxide biocomposite nanofibers. *J Ind Eng Chem* 20: 4415–4420.
30. Xu J, Zhang J, Gao W, et al. (2009) Preparation of chitosan/PLA blend micro/nanofibers by electrospinning. *Mater Lett* 63: 658–660.
31. Zhang H, Wu C, Zhang Y, et al. (2010) Elaboration, characterization and study of a novel affinity membrane made from electrospun hybrid chitosan/nylon-6 nanofibers for papain purification. *J Mater Sci* 45: 2296–2304.
32. Spasova M, Manolova N, Paneva D, et al. (2004) Preparation of chitosan-containing nanofibres by electrospinning of chitosan/poly (ethylene oxide) blend solutions. *E-Polymers* 4: 056.

33. Desai K, Kit K, Li J, et al. (2008) Morphological and surface properties of electrospun chitosan nanofibers. *Biomacromolecules* 9: 1000–1006.
34. Mengistu Lemma S, Bossard F, Rinaudo M (2016) Preparation of pure and stable chitosan nanofibers by electrospinning in the presence of poly (ethylene oxide). *Int J Mol Sci* 17: 1790.
35. Ohkawa K, Cha D, Kim H, et al. (2004) Electrospinning of chitosan. *Macromol Rapid Comm* 25: 1600–1605.
36. Ohkawa K, Minato KI, Kumagai G, et al. (2006) Chitosan nanofiber. Biomacromolecules 7: 3291–3294.
37. Nirmala R, Il BW, Navamathavan R, et al. (2011) Preparation and characterizations of anisotropic chitosan nanofibers via electrospinning. *Macromol Res* 19: 345.
38. Nirmala R, Navamathavan R, El-Newehy MH, et al. (2011) Preparation and electrical characterization of polyamide-6/chitosan composite nanofibers via electrospinning. *Mater Lett* 65: 493–496.
39. Geng X, Kwon OH, Jang J (2005) Electrospinning of chitosan dissolved in concentrated acetic acid solution. *Biomaterials* 26: 5427–5432.
40. Homayoni H, Ravandi SAH, Valizadeh M (2009) Electrospinning of chitosan nanofibers: Processing optimization. *Carbohyd Polym* 77: 656–661.
41. Ibrahim HM and Klingner A (2020) A review on electrospun polymeric nanofibers: Production parameters and potential applications. *Polym Test* 90: 106647.
42. Rinaudo M, Milas M, Le Dung P (1993) Characterization of chitosan. Influence of ionic strength and degree of acetylation on chain expansion. *Int J Biol Macromol* 15: 281–285.
43. Tan SC, Khor E, Tan T K, et al. (1998) The degree of deacetylation of chitosan: advocating the first derivative UV-spectrophotometry method of determination. *Talanta* 45: 713–719.
44. ASTM D1125-14 (2014) Standard Test Methods for Electrical Conductivity and Resistivity of Water, ASTM International, West Conshohocken, PA.
45. Viera DF, Avellaneda CO, Pawlicka A (2008) AC impedance, X-ray diffraction and DSC investigation on gelatin based-electrolyte with LiClO4. *Mol Cryst Liq Cryst* 485: 843–852.
46. Shukur MF, Majid NA, Ithnin R, et al. (2013) Effect of plasticization on the conductivity and dielectric properties of starch–chitosan blend biopolymer electrolytes infused with NH_4Br. *Phys Scr* 2013: 014051.
47. Bossard F and Rinaudo M (2019) Biomaterials from chitosan processed by electrospinning. *Nanoworld J* 5: 32–35.
48. Li Q, Song B, Yang Z, et al. (2006) Electrolytic conductivity behaviors and solution conformations of chitosan in different acid solutions. *Carbohyd Polym* 63: 272–282.
49. Andrady AL (2008) *Science and Technology of Polymer Nanofibers*, New Jersey: John Wiley & Sons.